Politecnico di Torino

Université Paris Cité

Device for the Identification of Airborne Chemical Agents by Enhanced Raman Spectroscopy

Marco Ciaramella

Tutor: Simon Delacroix

03 March 2022 – 29 July 2022

Acknowledgements

I would like to thank Yvan Bonnassieux and Aleix Guell for welcoming me to the PICM laboratory.

I would like to thank Thierry Gacoin for his welcome to the PMC laboratory as well as all the members of the PMC laboratories for their warm welcome.

I would like to thank Simon, a friend before a tutor, for the support he has provided me in the challenges of research and life, for his constant patience and for being a model as a researcher and as a man.

Finally, I would like to thank Maria Luisa Della Rocca, affectively called “Mamma Luisa” among the DQ Master guys, for her constant presence in the slip moments of this wonderful Erasmus program.

I would like to thank Salvatore, Giovanni, Samuele, and all the friends who someway supported me along the way even without knowing.

I would like to thank the Erasmus buddies, we grew up together becoming a family, I won’t forget none of you.

I would like to thank Martina, Claudia, Jacopo, Emilio and all the Fapcom friends, that are my second family, for motivating me to chase my ambitions. You all are a reference point of my life.

I would like to thank Lusio, Luca and Riccardo, I wouldn’t be here without you guys. Thanks for the notes, for the nights spent studying together, for the laughs and for the constant sharing of anxieties and uneasiness.

I would like to thank Crisà, sorry but I will never call you Francesco. Thanks for the calm and the serenity you are able to provide me just smiling, for the advice that guided me in-between bad times, for being constantly by my side, for being my best friend.

I would like to immensely thank my parents, even if you are completely inadequate to understand the problems of a student, I felt all the love you put in the effort of hold me up day-by-day. There are no words to express how much I feel lucky to have such two columns protecting my back. I love you so much.

I would like to thank myself, well-done man. You never gave up, I’m proud of what you became.

Lastly to you, I miss you infinitely.

Index

Abbreviation table

Abbreviation	Signification
MOF	Metal-Organic Framework
SERS	Surface Enhanced Raman Spectroscopy
NP	Nanoparticle
NBP	Nanobipyramid
NS	Nanosphere
NR	Nanorod
X@Y	Core-Shell structure of X as core and Y as shell
X:Y	Composite structure of X and Y
SEM	Scanning Electron Microscope
TEM	Transmission Electron Microscope
XRD	X-Ray Diffraction
EDX	Energy-Dispersive X-Ray Spectroscopy
VOC	Volatile Organic Compound
EM	Electro-Magnetic
RPM	Rounds Per Minute

1. Introduction

Starting from the 3rd of March, I started my M2 internship at the Ecole Polytechnique in the laboratories of Physics of Condensed Matter (PMC) and Physics of Interfaces and Thin Layers (PICM). The subject of the internship is the manufacturing of devices capable to sense VOCs exploiting Raman spectroscopy.

1.1 Presentation of the laboratories

PICM and PMC are part of the 23 scientific laboratories of the Ecole Polytechnique. PICM is a multidisciplinary laboratory where fundamental research in the fields of materials science, chemistry, electronics and optics is developed. Different applications are targeted as the production and storage of photovoltaic energy, nanostructured new sensors using organic and inorganic materials. PMC is organized into four research groups: the Physics of Irregularity and Confined Environments group, which is interested in the influence of geometric irregularities on morphogenesis and transport dynamics, the Electrons-Photons-Surfaces group is interested in the optical properties of surfaces, especially those of semiconductors, the Electrochemistry and Thin Films group is interested in the physics and chemistry of surfaces and interfaces, studying them with an electrochemical approach, and lastly the Solid State Chemistry group is interested in the preparation and study of inorganic nanomaterials.

It is just within the PMC and PICM laboratories that I'm doing my internship under the direction of Simon Delacroix as tutor and Aleix Guell as project director.

1.2 Internship subject and goal

Volatile Organic Compounds (VOCs) are organic molecules (butane, toluene, ethanol, acetone, benzene, etc…), generally derived from oils, with high vapor pressure at room temperature, that can be therefore easily found in its vapor phase under atmospheric pressure conditions. VOCs are known to be markers of air quality since they strongly impact on ozone cycle and greenhouse effect. Moreover, some of them belong to the CMR (carcinogenic, mutagenic and reprotoxic) chemicals being hence very dangerous for the human health, and in certain specific cases they can also reveal the presence of explosive substances and drugs. As a consequence of the aforementioned reasons, the detection of these compounds turns out to be crucial for numerous applications in the ecology, human health, and security fields. In order to match the requirements of the future sensors in terms of speed, cost and selectivity, Raman spectroscopy seems to be the perfect analytic tool. Indeed it is fast, inexpensive and also selective since the Raman signal contains the vibrational fingerprint of each molecule . Despite that, this technique lacks of sensitivity, indeed the Raman response of diluted gaseous VOCs is usually very low and difficult to detect. Therefore, my internship is oriented to try to face and overcome this technological issue by developing new materials for VOCs sensing.

Two strategies have been taken in consideration in order to develop new sensors based on Raman spectroscopy. The first one is based on Surface Enhanced Raman Spectroscopy (SERS)[1]. Indeed, a substance interacting with a substrate having plasmonic properties shows an increase of its own Raman signal, assuming the plasmonic resonances to be excited by lasing light at proper wavelength (Figure 1.A). In this work, I have chosen to use gold plasmonic nanoparticles (NPs) since they are more chemically stable with respect to other metallic NPs, moreover their size and morphologies can be easily tuned[2,3]. It is interesting to work with different morphologies since each of them has distinct plasmonic resonances, whose features as for example spatial confinement, affect their enhancement factor of the VOCs Raman signal. Moreover, while some morphologies act better when isolated, others benefit of an increasing of the enhancement factor when organized together. During my internship, I have mainly worked with Au NanoSpheres (NSs) and Au NanoBiPyramids (NBPs) but also Au NanoRods (NRs). The second strategy consists of using porous compounds, namely Metal Organic Frameworks (MOFs). These porous three-dimensional hybrid networks are made of an inorganic part which could be a metallic cation or a metallic cluster and an organic ligand. The MOFs will allow the local increase of the VOCs concentration by trapping them into their pores.

Furthermore, the rich MOF chemistry enable a selective absorption of the analyte (Figure 1.B). Indeed, based on the metal ions/clusters and the organic ligands the MOF is made of, the porosity can be tuned, as well as the surface functionalization groups that make a MOF hydrophilic or hydrophobic. Depending on these features, each MOF is more prone to host certain compound than others. During my internship, I worked with ZIF-8 and UiO-66(NH_2)[4,5]. The choice of these two MOFs is due to their properties, in fact ZIF-8 is easy synthesizable and UiO-66(NH_2) is chemically stable. Furthermore, ZIF-8 being hydrophobic due to its imidazole linkers, and UiO-66(NH_2) hydrophilic due to the NH_2 functional group, VOCs with different chemistry can be equally sensed.

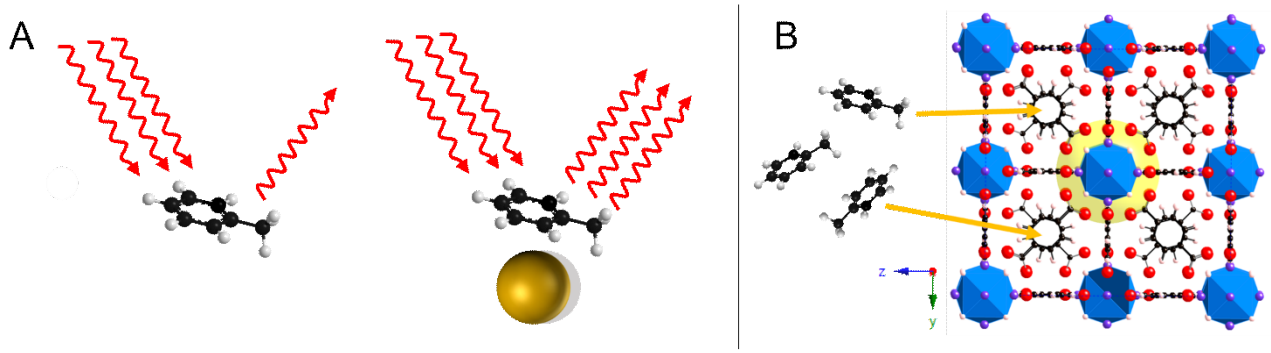

Figure 1. (A) Schematic of SERS principle, (B) Schematic of VOC capturing through a MOF.

Finally, the two strategies can be combined to push the detection limit of new sensors[6–8]. Indeed, substrates made of MOFs and Au-NPs will concentrate the analytes in the vicinity of the plasmonic surface, aiming to be the perfect candidates to compensate the lackness of sensitivity of the VOCs sensing through Raman spectroscopy. The combination of MOF and Au NPs is approached in two different ways, either exploiting the concept of core-shell nanostructure or by simply mixing the NPs separately in composites (Figure 2). In a core-shell NP a layer of MOF will surround the Au core, whereas in the composites MOF and Au will be distinct NPs. Therefore, the goal of my internship is to develop a functional VOCs sensor based on innovative substrates made of gold and MOFs particles.

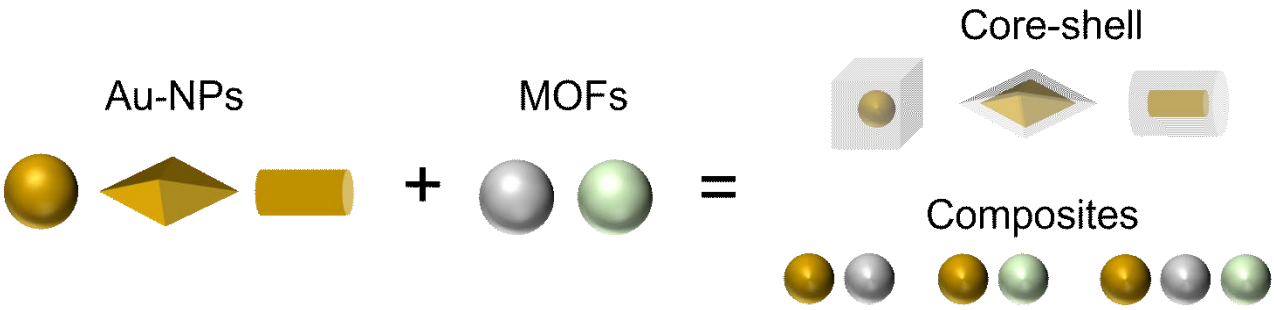

Figure 2. Schematic of the embedding of the SERS and MOF functionalities in different configurations.

In literature the idea to combine SERS and MOFs for gas sensing has been investigated only during the last ten years. Usually, thick corrugated films of gold or silver particles are covered by a layer of MOFs[9–11]. A more promising approach would be to use different populations of gold and MOFs nanoparticles or even better, core-shell particles to develop new innovative sensors[6–8]. This approach is beginning to be studied but for the moment, only the ZIF-8 structure was studied. Thus, it would be of a great interest to generalize this approach to new MOF like UiO-66. Furthermore, the rare studies reported in the literature do not make a serious comparison between the different sensor configurations.

In a first part of this report, I will present the synthesis and characterization of MOFs and core-shell particles. In a second part, I will present the shaping of new substrates based on the previous particles. Finally, the sensing properties for VOCs detection of the different substrates will be evaluated in the last part of this report.

2. Results

2.1 Synthesis and Characterization of Nanoparticles

In this part, the synthesis of the ZIF-8, the UiO-66(NH_2) and the core-shell Au@ZIF-8 NPs is treated (Appendix I. Synthesis). The NPs are characterized by various techniques (Appendix II Characterization) in order to retrieve their main features, in particular size dispersion and crystallinity.

2.1.1 ZIF-8

ZIF-8, standing for Zeolitic Imidazolate Framework-8, is one of the most studied MOF due to its properties, in particular easy synthesis. This MOF has been chosen to be used both for the aforementioned properties, but mainly because it is suitable to host toluene, which will be the model VOC in this study, either in terms of pore size or hydrophobicity. Its structure is composed of Zn tetrahedrons connected by imidazolate linkers (Figure 3A). Nanoparticles of ZIF-8 are obtained by colloidal synthesis starting from zinc nitrate and 2-Methylimidazole stirred in methanol during one hour at room temperature (Equation 1)[12]. The NPs are isolated by centrifugation and redispersed in ethanol.

$$Zn(NO_3)_2.6H_2O + \text{2-MeImdz} \xrightarrow[1h,\ RT]{MeOH} \text{ZIF-8}$$

Equation 1. Colloidal synthesis of ZIF-8.

The crystallinity and the NPs size are important characteristics. Indeed, a poor crystallinity would involve a poor alignment of the pores of the network, that would cause a slow diffusion of the analyte in the MOF, reducing its diffusion performances. The NPs size is also a critical factor, indeed the enhancement effect of Au-NPs is localised in the tenth of nm surrounding the surface plasmonic resonances. Hence, too big MOF NPs would lead to the analyte concentration in a space region not affected by EM field enhancement. In order to investigate these features, NPs are dried at 80°C during 2h and characterized by transmission electronic microscopy (TEM), X-Ray diffraction (XRD) and Raman spectroscopy. According to the XRD spectrum (Figure 3B), the ZIF-8 particles are crystalline and according to the TEM NPs have an average diameter of 44 nm (Figure 3C). Raman spectrum of the ZIF-8 powder confirms the obtention of the ZIF-8 phase (Figure 3D).

2.1.2 UiO-66(NH_2)

UiO-66(NH_2), UiO standing for University in Oslo where this MOF was synthesized for the first time, is a zirconium-based MOF known for its high thermal and chemical stability[13]. Its structure is composed of $[Zr_6O_4(OH)_4]^{12+}$ zirconium clusters connected by 2-aminoterephthalate anions (BDA-NH_2, Figure 4.A). The chemistry of the UiO-66 MOFs is very versatile. Indeed, by change the functional groups on the benzene ring in the organic linker, the chemical properties of the UiO-66 can be easily tuned. UiO-66(NH_2) results to be highly hydrophil thanks to the NH_2 functional group. This feature, in opposition to the hydrophobicity of ZIF-8, allow for the in-pores hosting of substances as ethanol and acetone. The synthesis of this MOF is performed through a 2-step process (Equation 2)[4,5,14]. First, the synthesis of the zirconium clusters surrounded by acetate $CH_3CO_2^-$ ligands is performed by reflux of the $ZrCl_4$ salt in isopropanol in presence of acetic acid. The clusters are isolated by centrifugation and dried. In the second step, the clusters are mixed with the organic linker BDA in ethanol during two hours at room temperature in presence of acetic acid. In this second step, the addition of acetic acid is of primary importance since this molecule is terminated by a carboxilate group. In fact, the BDA linker presents also this termination. The competition of this two chemical species in saturating the zirconium clusters bonds (since acetate groups are now dissolved in ethanol), let the network grow slowly allowing the proper crystallization of the 3D framework (Figure 4.A)[15].

1 $ZrCl_4$ + Acetic Acid $\xrightarrow[\text{Reflux, 2h}]{\text{iPrOH}}$ $[Zr_6O_4(OH)_4(CH_3CO_2)_{12}]$

2 $[Zr_6O_4(OH)_4(CH_3CO_2)_{12}]$ + BDC-NH_2 $\xrightarrow[\text{Acetic Acid}]{\text{EtOH, } H_2O}$ UiO-66(NH_2)

Equation 2. Colloidal synthesis of UiO-66(NH_2).

As already mentioned for ZIF-8, two paramount features of MOF NPs are crystallinity and diameter dispersion. Hence, after the synthesis a certain amount of NPs is dried at 80°C during 2h and characterized by transmission electronic microscopy (TEM), X-Ray diffraction (XRD) and Raman spectroscopy. The crystallinity of the particles is confirmed by XRD and Raman spectroscopy (Figure 4.B, Figure 4.D). The average size of the UiO-66(NH_2) particles is around 35 nm (Figure 4.C). The two-step reaction using preformed cluster allow a growth a room temperature. This synthesis strategy separating the nucleation and the growth step decrease the growth rate and allow the formation of small nanoparticles.

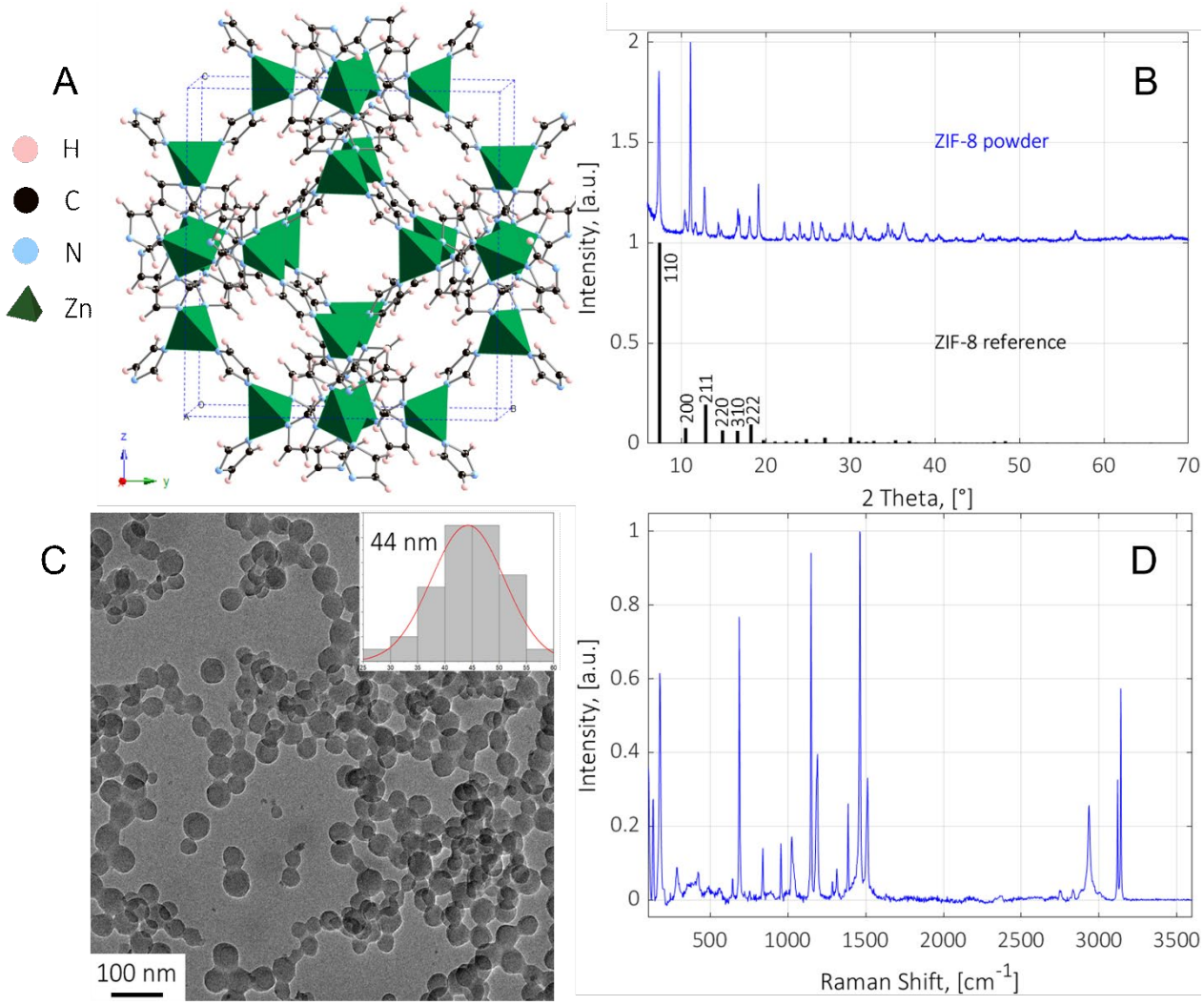

Figure 3. (A) 3D structure of ZIF-8, (B) ZIF-8 XRD spectrum, (C) ZIF-8 NPs TEM picture, (D) ZIF-8 Raman spectrum.

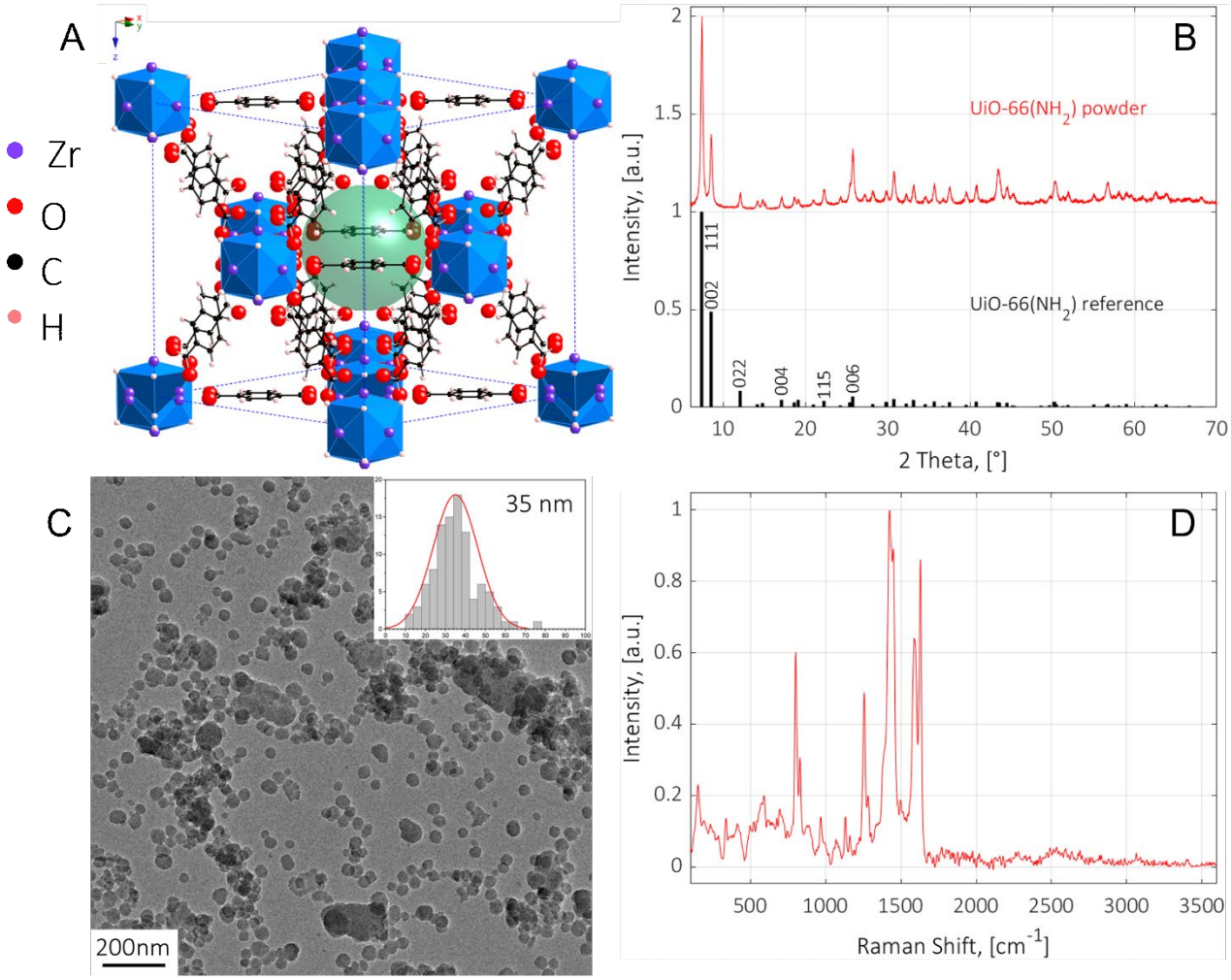

Figure 4. (A) 3D structure of UiO-66(NH_2), (B) UiO-66(NH_2) XRD spectrum, (C) UiO-66(NH_2) NPs TEM picture, (D) UiO-66(NH_2) Raman spectrum.

2.1.3 Au-Nanobyparamids and ZIF-8 Core-Shells

Core-shell structures gained lot of attention in the last decades due the possibility to embed more and more properties in a single NP, as for example the active manipulation by means an external field, the optical imaging with fluorescence, the electrical passivation, the biocompatibility, the functionalization with a specific targeting group, etc… During my internship I synthetized core-shell NPs using Au-NBPs as core and ZIF-8 MOF as shell. The NBPs have been previously synthesized by my tutor. These particles could be particularly interesting for trapping VOCs inside the ZIF-8 shell in the vicinity of the gold core to benefit from the SERS effect. The synthesis of Au-NBPs@ZIF-8 is performed through a multi-step process as follows: ZIF-8 precursors are stirred together with a surfactant (cetyltrimethylammonium bromide, CTAB) at room temperature. After 5 minutes, the gold NBPs are introduced in the reaction medium to grow the shell on it. Then the mixture is left without stirring during 1h at room temperature and the growth is stopped by removing the precursor leftovers in solution by means of cleaning processes (Equation 3). Since one could think that the MOF will grow in NPs separately from the Au-NPs, it must be specified that the growth of the shell occurs because of the minimization of the surface energy. Indeed, because of this phenomenon, the growth of the shells is favoured with respect to the nucleation and growth of MOF NPs alone.

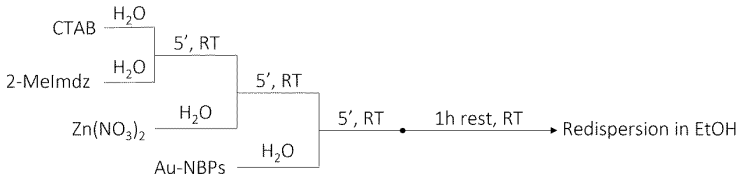

Equation 3. Colloidal synthesis of Au-NBPs@ZIF-8.

After the synthesis, the Au@NBPs are characterized by means of TEM and XRD. TEM imaging shows that the NBPs have a very good ZIF-8 coverage on their surface (Figure 5.A). It can also be noticed that, despite the core-shell structure is energetically favoured, some MOF NPs are synthetised because of homonucleation. This is due to the fact that the kinetic of the shell growth and the concentration of MOF precursors strongly affect the whole process, therefore the homonucleation of MOF NPs is difficult to be totally avoided. In Figure 5.B the average sizes of Au@NBPs are shown. The crystallinity of gold and in particular of the grown ZIF-8 shell is confirmed by the XRD spectrum (Figure 5.C).

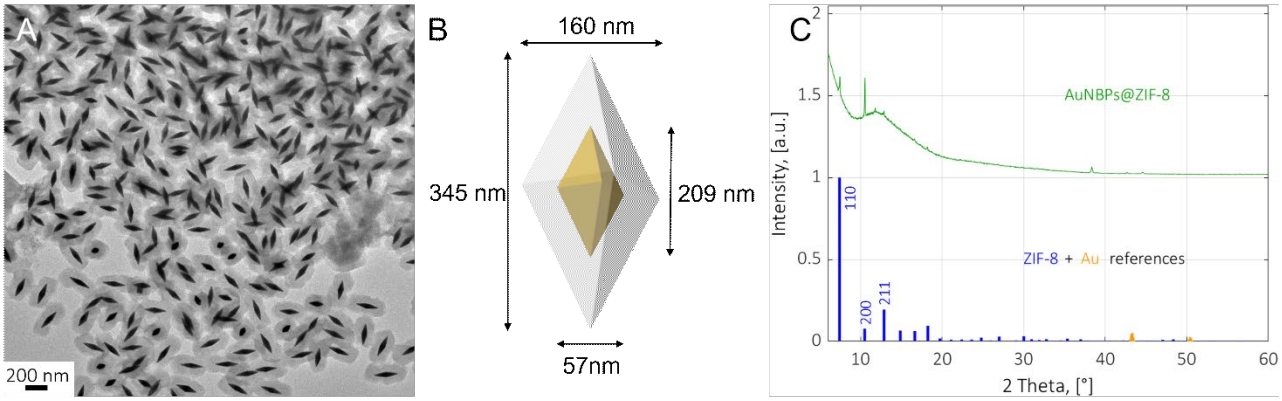

Figure 5. (A) TEM picture of Au-NBPs@ZIF-8, (B) Schematic of Au-NBPs@ZIF-8 sizes dispersion, (C) Au-NBPs@ZIF-8 XRD spectrum.

2.2 Preparation and characterization of SERS substrates

The NPs previously synthetized have to be dried to prepare samples capable to capture the VOCs from the surrounding atmosphere and perform SERS sensing. A silicon wafer (400) is chosen as substrate in this work, since its properties are well known either in terms of XRD spectrum or Raman spectrum. Moreover, being this crystalline plane easy cleavable in squares, this substrate is suitable to be used for our purposes. Indeed, square Si substrates with a constant area of $1cm^2$ are prepared on which the NPs are drop-casted. Drop-casting is chosen as deposition technique since, in order to be able to make quantitative comparisons between different samples, the aim is to have a controlled amount of Au-NPs on each sample Therefore, techniques such as spin coating or spray coating would have foreseen to lose part of the solution, being not suitable to deposit a controlled amount of solution. Instead, deposition through droplets allow for the control of the quantity of deposited solution. Clearly, in order to achieve a homogeneous deposition (on the scale of the laser spot), the solution must span the whole substrate covering it entirely. Hence, after ultrasound cleaning in acetone and anhydrous ethanol, the substrates undergo ozonolysis, such that the substrate surface is made hydrophilic (Figure 6). In this way the deposited solution will cover almost entirely the substrate while drying, making the NPs thin layer quite homogenously deposited and therefore also the local NPs concentration constant.

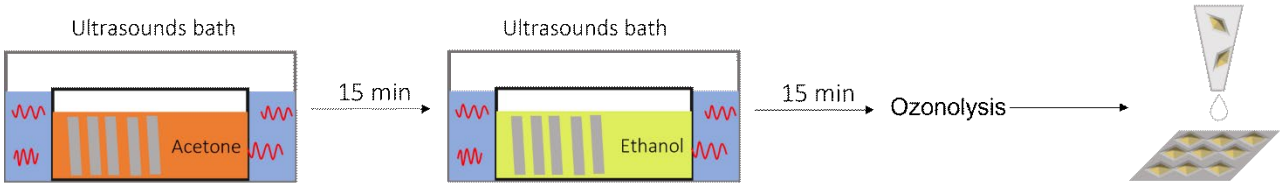

Figure 6. Schematic of substrate cleaning and droplet deposition.

2.2.1 Au-NPs

Au-NPs, already synthetized before my arrival, are deposited since they will have the role of reference (together with the MOF) to validate the advantages provided by the use of both the Raman enhancing strategies. Moreover, from the literature it is known that NPs shapes that usually perform greatly in enhancing the Raman signal alone, are less performant when arranged together. This phenomenon paves the way for the investigation about which shape (and size) will perform better for our sensing purposes.

2.2.1.1 Au-NSs

Au NSs were originally dispersed in water and previous depositions showed that they are not so concentrated, indeed poor coverages of the substrates were observed. Hence, to increase the concentration NPs are centrifugated for 15 minutes at 10^4 rounds per minute (rpm) and then redispersed in a smaller volume of ethanol in order to concentrate them of a factor 10, but still avoiding aggregation. After that, they are deposited as explained and then left to dry. At the end, the sample has been characterized through SEM imaging (Figure 7). The NSs organise themselves in islands that are quite uniformly dispersed on the substrate, paving the way for non-spot dependent Raman measurements.

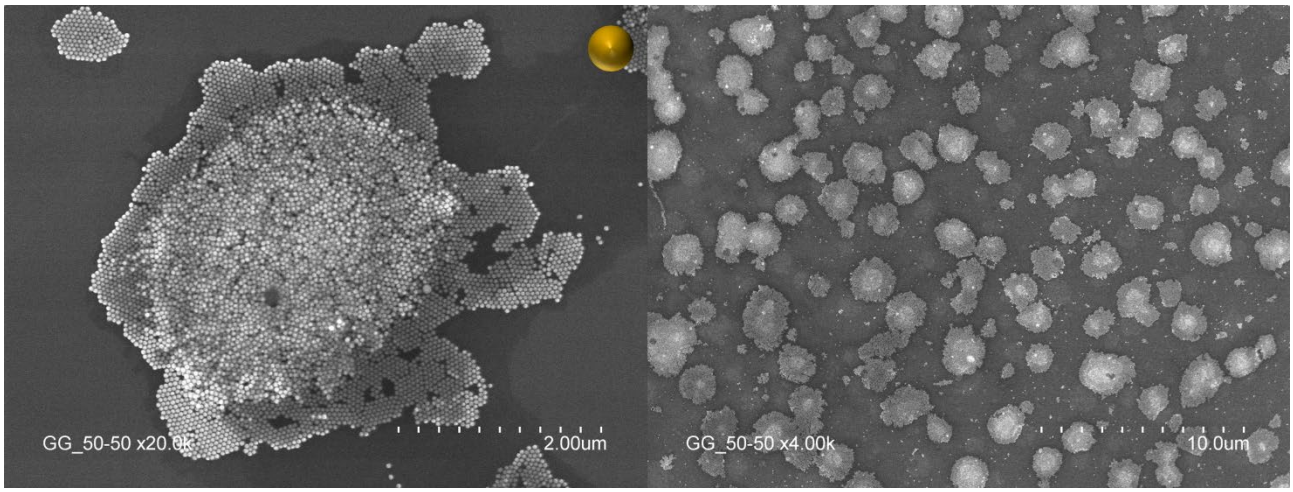

Figure 7. SEM pictures of droplet-deposited Au-NSs on a Si substrate.

2.2.1.2 Au-NBPs

Au-NBPs were originally dispersed in water and previous depositions showed that they are not so concentrated, indeed poor coverage of the substrates was observed. Hence, as well as the Au-NSs, to increase the concentration NPs are centrifugated for 15 minutes at 10^4 rpm and then redispersed in a smaller volume of ethanol in order to concentrate them of a factor 10, but still avoiding aggregation. After that, they are deposited as explained and then left to dry. SEM imaging (Figure 8) show that also NBPs tend to organize themselves in islands which are quite uniformly dispersed on the substrate surface. It should be noticed how the NBPs seem to be randomly orientated into the islands, avoiding polarization effects that would have led to different enhancement factors for the SERS depending on the laser polarization. Another evidence that must be pointed out is that not all the NPs seem to be NBPs. Despite that, they seem to be a low percentage and their presence can be neglected.

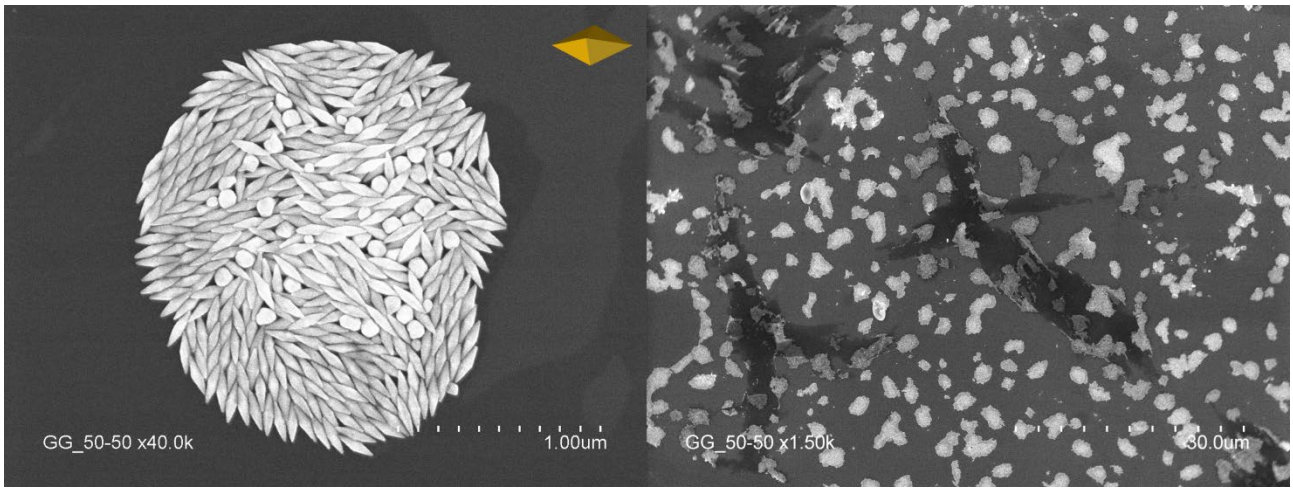

Figure 8. SEM pictures of droplet-deposited Au-NBPs on a Si substrate.

2.2.2 MOFs

MOFs, entirely synthetized by me as illustrated in the previous subsections, are of great interest in being deposited since they will have the role of reference as well as the Au-NPs. In the following both ZIF-8 and UiO-66(NH_2) are treated.

2.2.2.1 ZIF-8

ZIF-8 NPs, produced as illustrated in subsection 2.1.1, are deposited as explained and then characterized through SEM imaging (Figure 9). It can be noticed that the substrate coverage is very uniform, despite some cracks due to the sample drying.

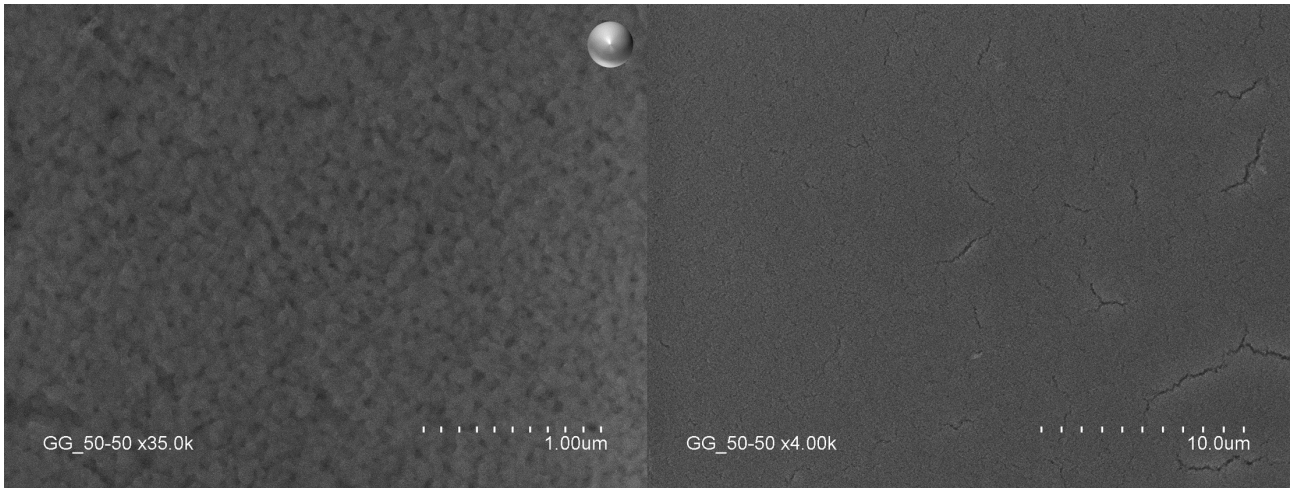

Figure 9. SEM pictures of droplet-deposited ZIF-8 NPs on a Si substrate.

2.2.2.2 UiO-66(NH_2)

UiO-66(NH_2) NPs, produced as illustrated in subsection 2.1.2, are deposited as explained and then characterized by means of SEM imaging (Figure 10). Also in this case, as for the ZIF-8, the good coverage of the sample can be appreciated, despite some cracks due to the solvent drying.

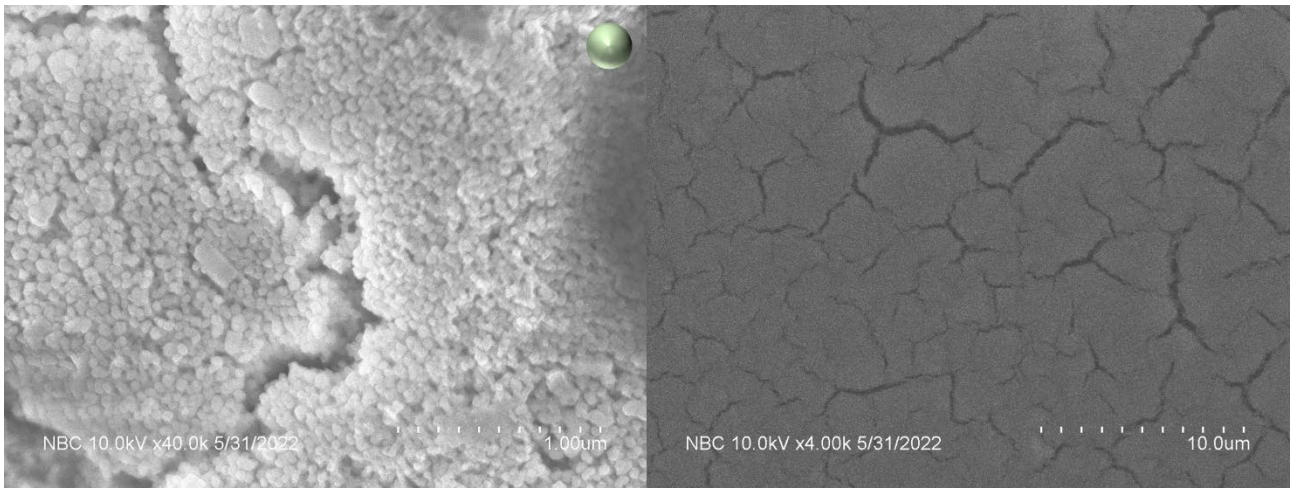

Figure 10. SEM pictures of droplet-deposited UiO-66(NH_2) NPs on a Si substrate.

2.2.3 Au@ZIF-8 core-shells

Core-shell NPs are of paramount importance to be accurately deposited, indeed they are the main focus of the project and receive the highest expectations in terms of results. Using ZIF-8, core-shell NPs have been synthetized for all shapes and sizes of Au-NPs. In the following, the deposition of Au-NSs@ZIF-8 and Au-NBPs@ZIF-8 are treated.

2.2.3.1 Au-NSs@ZIF-8

Au-NSs@ZIF-8 NPs, as well as the Au-NPs previously discussed, were originally dispersed in water and previous depositions showed that they are not so concentrated, indeed poor coverage of the substrates was observed. Hence, to increase the concentration they are centrifugated for 30 minutes at $11x10^3$ rpm and then redispersed in a smaller volume of ethanol to concentrate them of a factor 10, but still avoiding aggregation. Then the solution is deposited as explained and characterized by means of SEM imaging (Figure 11). It is worth to notice that the NPs are quite homogeneously dispersed on the substrate. Despite that lot of NPs do not contain any Au NP, because of the MOF homonucleation, and the SERS effect is therefore not granted anywhere.

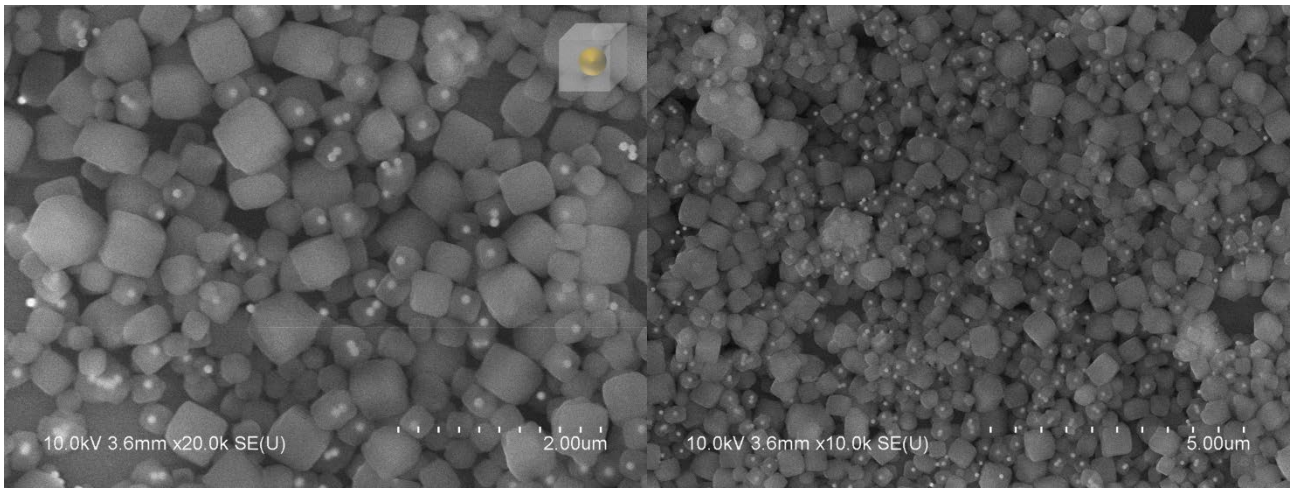

Figure 11. SEM pictures of droplet-deposited Au-NSs@ZIF-8 on a Si substrate.

2.2.3.2 Au-NBPs@ZIF-8

Au-NBPs@ZIF-8, produced as illustrated in subsection 2.1.3, were originally dispersed in ethanol and previous depositions showed that they are not so concentrated, indeed poor coverage of the substrates was observed. Hence, to increase the concentration they are centrifugated for 30 minutes at $11x10^3$ rpm and

then redispersed in a smaller volume of ethanol to concentrate them of a factor 10, but still avoiding aggregation. Then the solution is deposited as explained and characterized by means of SEM imaging (Figure 12). As shown, the NPs are quite homogeneously dispersed on the substrate, assuring properties consistency all over the sample.

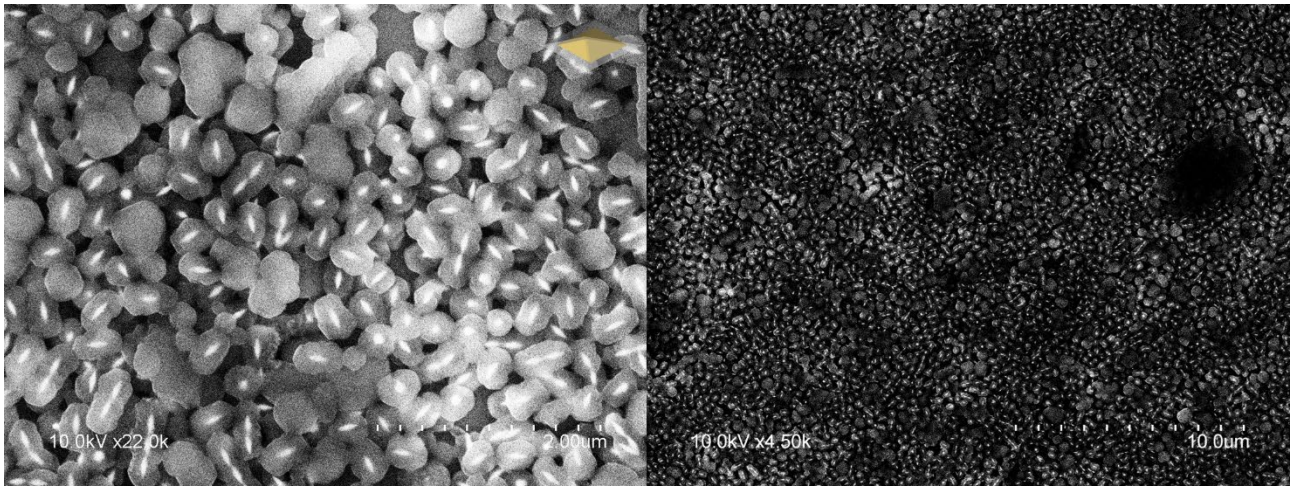

Figure 12. SEM pictures of droplet-deposited Au-NBPs@ZIF-8 on a Si substrate.

2.2.4 Au:MOF composites

Au:MOF composites are the other configuration, in addition to core-shell structures, that could allow the increase of the limit of detection of a sensor based on Raman spectroscopy. To achieve such substrates, different populations of gold and MOF are mixed and deposit on a Si surface. For what concerns our purposes, the big advantage in performing experiments with this configuration is the possibility to use UiO-66(NH_2) NPs in addition to ZIF-8 ones, paving the way for selectivity measurements. Furthermore, since the diameter size dispersions of Au NSs, ZIF-8 NPs and UiO-66(NH_2) NPs are all centred around 35-45nm, one of the perspectives is to obtain a 1:1 ratio between the Au NPs and MOF NPs. In such a configuration, every MOF NP will benefit from the SERS effect by means of the surrounding Au NPs. An optimization of the initial colloidal dispersion ratio was done. Moreover, it must be specified that for the Au:ZIF-8 this was even more difficult since the Au-NSs and the ZIF-8 tended to aggregate separately.

2.2.4.1 Au-NSs:ZIF-8

The Au-NSs:ZIF-8 composite is prepared by stirring for 1 hour at room temperature ZIF-8 NPs, produced as in subsection 2.1.1, and Au-NSs. Since previous depositions revealed that the final solution is not concentrated enough, to increase the concentration the solution is centrifugated for 15 minutes at $10x10^3$ rpm. Then the mixture is redispersed in a smaller volume of its own supernatant to concentrate it of a factor 10, but still avoiding aggregation. After that the solution is deposited as explained and left to dry. Finally, the sample is characterized through SEM imaging (Figure 13). In this sample both Au-NPs and ZIF-8 seem to be quite homogeneously dispersed.

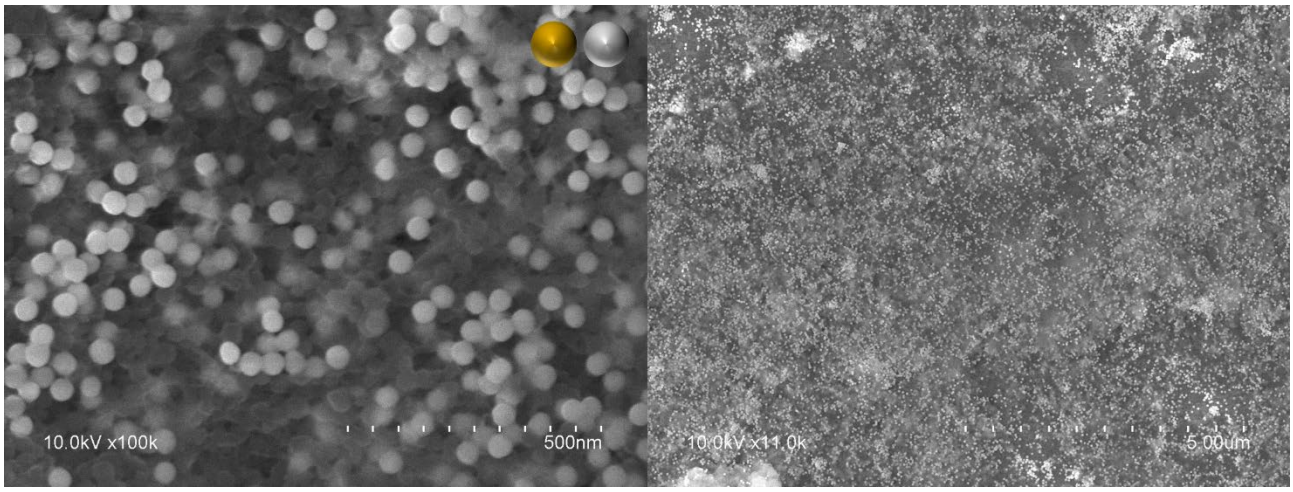

Figure 13. SEM pictures of droplet-deposited Au-NSs:ZIF-8 composite on a Si substrate.

2.2.4.2 Au-NSs:UiO-66(NH_2)

The composites Au-NSs:UiO-66(NH_2) composite is prepared by stirring for 1 hour at room temperature UiO-66(NH_2) NPs, produced as in subsection 2.1.2, and Au-NSs (synthetized before my arrival). Since previous depositions revealed that the final solution is not concentrated enough, to increase the concentration the solution is centrifugated for 15 minutes at $10x10^3$ rpm. Then the mixture is redispersed in a smaller volume of ethanol to concentrate it of a factor 10, but still avoiding aggregation. After that the solution is deposited as explained and left to dry. Finally, the sample is characterized through SEM imaging (Figure 14). One can appreciate how both Au-NPs and ZIF-8 seem to be quite homogeneously dispersed.

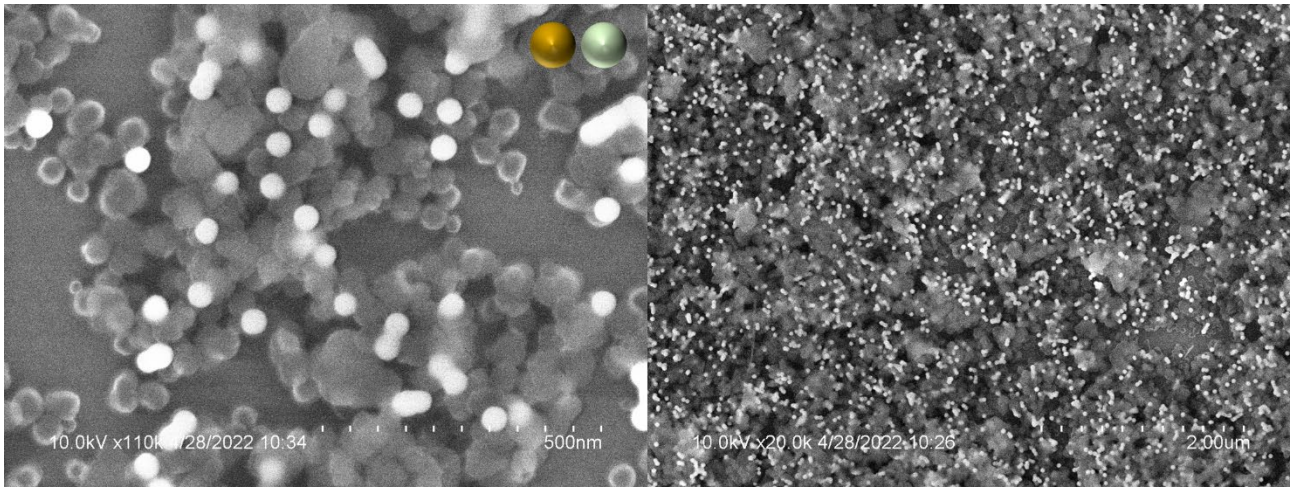

Figure 14. SEM pictures of droplet-deposited Au-NSs:UiO-66(NH_2) composite on a Si substrate.

2.2.4.3 Au-NSs:ZIF-8:UiO-66(NH_2)

In addition to the composites between Au NPs and ZIF-8/UiO-66(NH_2) taken separately, also a composite of Au NPs and both the MOFs together is realized. The aim of this sample is to achieve an "universal" sensor. Basically, as already explained, ZIF-8 is hydrophobic because of the imidazole organic linkers, whereas UiO-66(NH_2) is hydrophilic because of the NH_2 functional group on the network linkers. Therefore, the two MOFs have a chemical nature that allow them to host only certain VOCs. However, the perfect sensor must be sensitive to all the VOCs, hence in this composite both the MOFs are mixed together with Au NPs to make the final sample capable to trap VOCs with distinct chemistry. The Au-NSs:ZIF-8:UiO-66(NH_2) composite is prepared by stirring for 1 hour at room temperature ZIF-8 NPs, UiO-66(NH_2) NPs and Au-NSs. In order to increase the concentration, the solution is centrifugated for 15 minutes at $10x10^3$ rpm. Then the mixture is redispersed in a smaller volume of its own supernatant to concentrate it of a

factor 10, but still avoiding aggregation. After that, the solution is deposited as explained and left to dry. Finally, the sample is characterized through SEM imaging (Figure 16). It can be noticed that Au NSs and MOFs are quite homogeneously dispersed with respect to each other. Nevertheless, neither the NPs size nor the contrast help in distinguishing ZIF-8 from UiO-66(NH_2). Therefore, is still to be demonstrated their good dispersion in the sample. In order to check that, in the next month I will perform EDX on this sample. Indeed, being ZIF-8 and UiO-66(NH_2) MOFs based respectively on zinc and zirconium, the dispersion of these two elements can be evaluated.

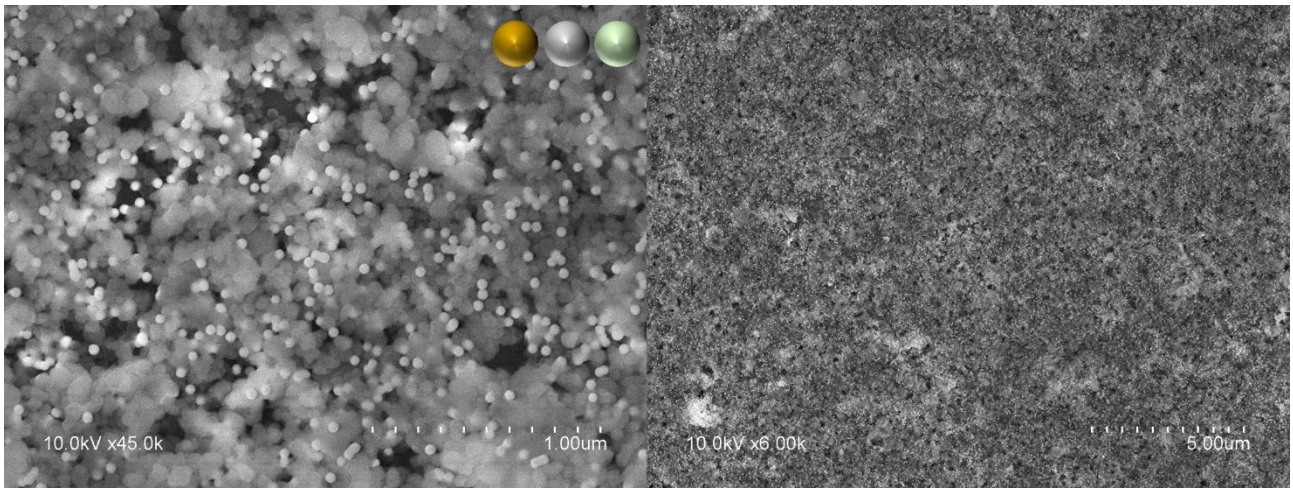

Figure 15. SEM pictures of droplet-deposited Au-NSs:ZIF-8:UiO-66(NH_2) composite on a Si substrate.

2.2.4.4 Au-NBPs:ZIF-8

The Au-NBPs:ZIF-8 composite is prepared by stirring for 1 hour at room temperature ZIF-8 NPs, produced as in subsection 2.1.1, and Au-NBPs. In order to increase the concentration, the solution is centrifugated for 30 minutes at $11x10^3$ rpm. Then the mixture is redispersed in a smaller volume of ethanol to concentrate it of a factor 10, but still avoiding aggregation. After that the solution is deposited as explained and left to dry. Finally, the sample is characterized through SEM imaging (Figure 12). In this sample both Au-NBPs and ZIF-8 seem to be quite homogeneously dispersed.

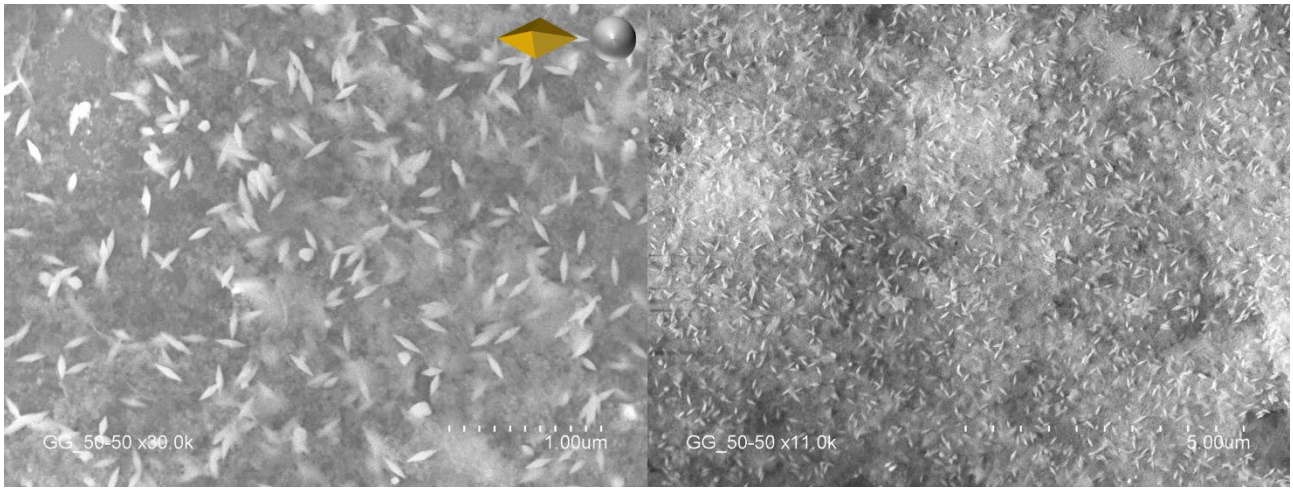

Figure 16. SEM pictures of droplet-deposited Au-NBPs:ZIF-8 composite on a Si substrate.

2.3 Volatile Organic Compounds detection

Once the samples are prepared, the goal is to study their VOCs sensing properties. The first information we want is purely qualitative and concerns the possibility to detect or not VOCs with substrates. Secondly, the idea is to go more in depth in the sensor characterization, trying to determine which sample is the best one in terms of sensibility, limit of detection and response time, focusing on demonstrate the advantages of the combination of the two enhancing approaches. Furthermore, from the literature it is known that the rich MOF chemistry enable a selective absorption of the analyte inside their pores. Indeed, based on the metal ions/clusters and the organic ligands the MOF is made of, the porosity can be tuned, as well as the surface functionalization groups that make a MOF hydrophilic or hydrophobic. Depending on these features, each MOF is more prone to host certain compound than others. During my internship, I worked with ZIF-8 and UiO-66(NH_2) that are, respectively, hydrophobic and hydrophilic, paving the way for selectivity measurements of different analytes. Lastly, reusability is one of the main features of a sensor, therefore the possibility of desorbing the analyte from the samples will be investigated. Since by detection it is meant the presence of the main peaks of the analyte in the acquired Raman spectrum, the target analyte must have at least one characteristic Raman peak that does not overlap with the ones of the used MOFs. Therefore, for the most part of the experiments, the used analyte is toluene (Figure 17).

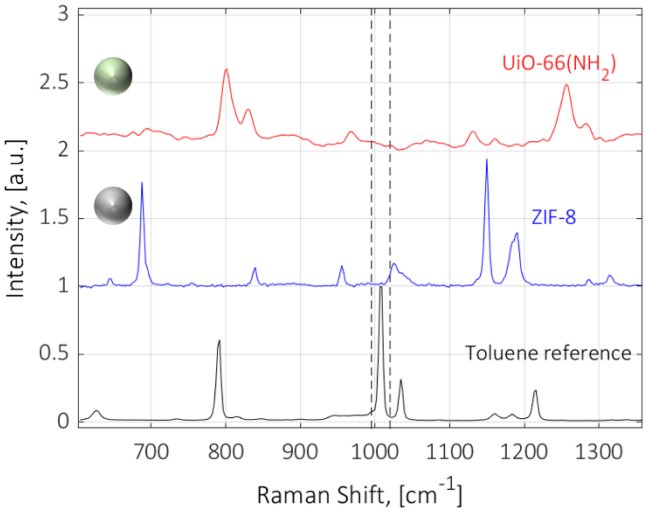

Figure 17. Toluene, ZIF-8 and UiO-66(NH_2) Raman spectra showing that the main peak of toluene does not overlap any of the MOFs ones.

2.3.1 Detection setup

The setup for the VOCs detection is a chamber represented in Figure 18. The chamber has as sample holder with a hot plate that allows to heat the substrates up to 650°C. Thanks to this chamber, VOCs detection can be carried out with two different approaches. The first approach is a static study of the samples sensing properties under saturated condition (Figure 18.A). In this configuration, the gas inlet and outlet that are sealed. A paper soaked with the analyte is introduced in the chamber in order to saturate the chamber atmosphere. The second possibility is to perform sensing under dynamic conditions by flowing a controlled atmosphere inside the chamber. For this purpose, the setup is completed by two voltage-controlled gas valves (Figure 18.B). One of them is simply assigned to the N_2 flow, whereas the other one makes some N_2 bubble in the liquid analyte. By controlling the ratio between these flows which are mixed just before to enter the chamber, the gaseous VOC concentration can be controlled inside the chamber. In this case, a career gas containing a certain amount of the analyte is flowed in the chamber. The sensing is then made *in operando* to test detection under conditions that are as close as possible to a real application condition of the sensor. Therefore, saturation conditions can be relevant only for first information about the VOCs detection, whereas for more precise information such as limit of detection, dynamic conditions must be evaluated.

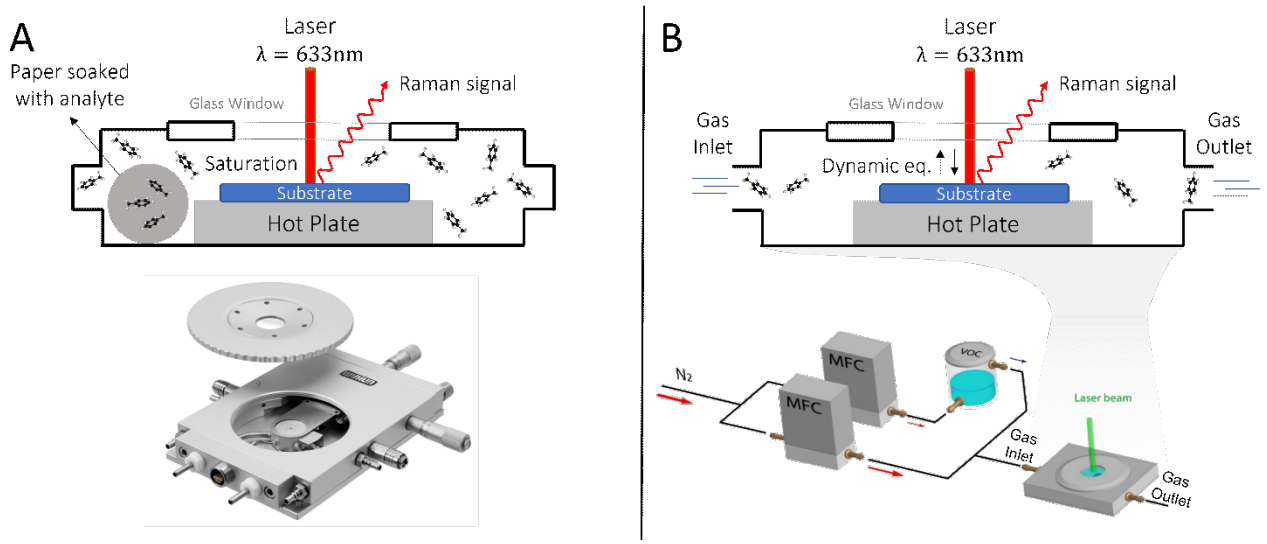

Figure 18. (A) Schematic of the static measurements setup, (B) Schematic of the dynamic measurements setup.

2.3.2 Static conditions

The purposes of a static study performed in saturation conditions is mainly to determine the capability to sense or not the analyte with different samples. Once this is done, the possibility to desorb the analyte starting from saturated conditions can be investigated as well. In order to ensure the saturation of the sample surface, some paper soaked with the target VOC is inserted in the chamber, which is then sealed. After a certain amount of time, experimentally determined for each sample by checking the amplitude of the main Raman peak of the analyte during over time up to its consistency, the substrate is saturated with the analyte. Under these conditions, the Raman spectrum of the different kind of substrates is acquired. In order to observe the presence of toluene the reference Raman spectrum of the substance has been acquired as well. Here it can be noticed that the main toluene peak is located at $\sigma = 1004$ cm^{-1}, as foreseen by literature (the peak at $\sigma = 520.8$ cm^{-1} is due to the Si substrate). Taking this peak as reference for the detection of toluene, it can be observed that in saturation conditions it is possible to detect it either with Au-NPs (either NBPs, or NSs, or NRs, Figure 19A), or Au-NPs@ZIF-8 core-shells, or Au-NPs:ZIF-8 composites, or ZIF-8 only, while we are not with a simple Si substrate (Figure 19B). It must be specified that the amplitude of the toluene main peak is meaningless since not properly re-normalized. Nevertheless, using the UV-VIS spectroscopy it would be possible to properly re-normalize the peak amplitude with respect to the absorbance (Appendix III. UV-Visible spectra of gold dispersions). Finally, it can be definitely said that this is the proof of concept of my work, basically while it is not possible to detect toluene with pure silicon, instead it is exploiting both the two approaches I considered. Nevertheless, this is true for saturated conditions, not exactly a diluted gaseous condition. We are now interested in the possibility to desorb the analyte in order to reuse the substrate for other measurements, and after that to check for the toluene detection in dynamic conditions.

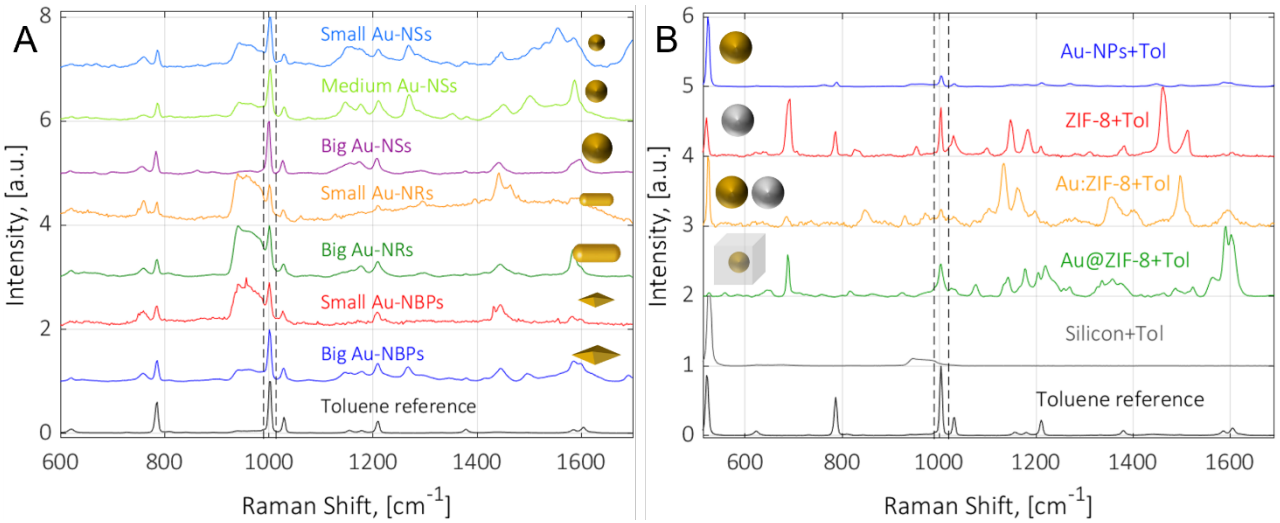

Figure 19. (A) Raman detection of toluene with differently shaped and sized Au-NPs, (B) Raman detection of toluene with Au-NPs, ZIF-8, Au-NSs@ZIF-8 and Au-NSs:ZIF-8.

2.3.2.1 Analyte desorption

As already outlined, an important feature for a sensor is surely the reusability. As consequence, one must be able to fully desorb the analyte from any kind of sample in order to allow for another detection, without contamination of any of the previously detected analytes. Here, the desorption study is included in the saturation condition treatment since, if is possible to desorb a fully saturated sample, it would also be possible for an unsaturated one. In particular, it is interesting to check the desorption for sample that contain MOFs. In fact, an analyte would be absorbed on a pure Au-NPs only by means of surface forces, that can be more easily overcome with respect to the ones that literally trap the analyte in the MOF pores. If the chamber remains sealed a dynamic equilibrium among the sample and the chamber atmosphere is established being the quantity of toluene fixed. Hence, the idea is to flow a pure N_2 flow that will continuously shift the equilibrium by removing the toluene in the chamber atmosphere allowing the desorption of the analyte from the sample. If this would not be enough to totally desorb the analyte, another idea is surely to heat up the substrate using the hot plate embedded in the chamber. In fact, a temperature increasing would increase the volatility of the analyte, helping its desorption.

The results of the first desorption test at room temperature with a previously saturated Au-NSs@ZIF-8 substrate are shown in Figure 20.A (blue curve). The amplitude of the toluene peak at σ = 1004 cm^{-1} decreases very slowly and after 6 hours toluene is not fully desorbed from the MOF pores. Further desorption tests are made with increasing the substrate temperature at 50, 100 and 150 °C to increase the desorption rate. The stability of the substrate and especially of the ZIF-8 is followed by XRD and Raman spectroscopy (Figure 20.B, Figure 20.C). At least until 150°C the ZIF-8 is stable, but at 200°C despite the XRD keeps confirming the crystallinity, the Raman spectrum shows the appearance of new broad peaks, originally not predicted by the ZIF-8 reference spectrum. This experimental observation is a marker of the loss of ZIF-8 chemical structure, limiting our possibilities to heat substrates containing ZIF-8. In Figure 20.A they can be seen the desorption curves at 50, 100 and 150°C (red and green and olive curves), showing that, even at 150°C, after 6 hours toluene is not fully desorbed from the MOF pores. This problem can be related to one issue we have recently found in our setup. Indeed, we discovered that the setup pipes are prone to adsorb toluene, then releasing it when pure N_2 is flowed through them. This implies the permanent presence of analyte in the atmosphere, probably leading to the impossibility to totally empty the substrate. Now I moved to more chemically inert Teflon pipes, with which will be possible to avoid this issue.

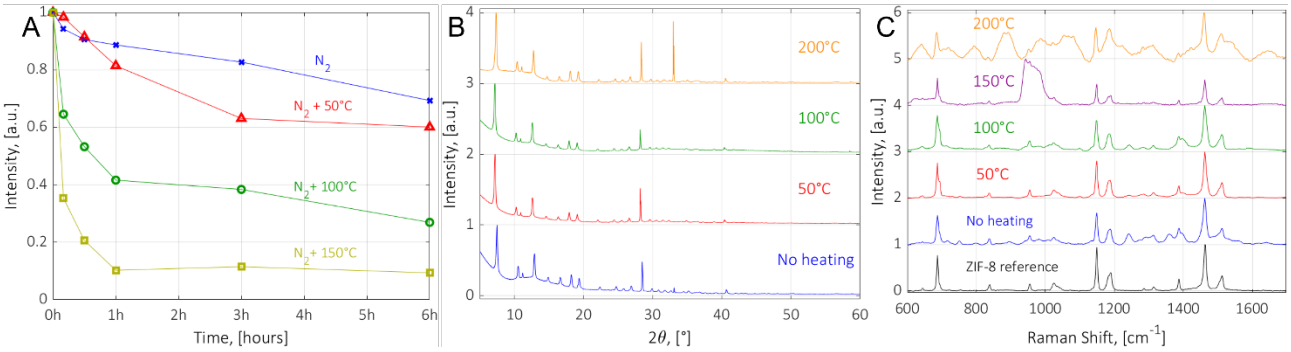

Figure 20. (A) Toluene desorption curves at different temperatures, (B) XRD spectra of ZIF-8 after heating at different temperatures, (C) Raman spectra of ZIF-8 after heating at different temperatures.

Concerning asymmetric Au-NPs, one of the evidence in literature is the reshaping towards spherical symmetry when they are heated up. Therefore, being our analyte desorption supported by heating, it is of interest to check for the presence of this phenomenon. In our experiments, performed with Au-NBPs both alone and as core of a core-shell structure, it is observed that the presence of the shell is able to preserve the asymmetric shape of the NPs. Figure 21.A shows the *post-mortem* SEM imaging of Au-NBPs@ZIF-8 that have been submitted to 150°C heating for 6 hours. It can be noticed that the NBPs are still properly shaped. On the other hand, in Figure 21B the *post-mortem* SEM imaging of Au-NBPs that have been submitted to 50°C heating for 2 hours is reported. It is clearly noticeable the rounding of the NBPs towards spherical shape. This evidence already provides a reason to prefer core-shells to Au-NPs alone.

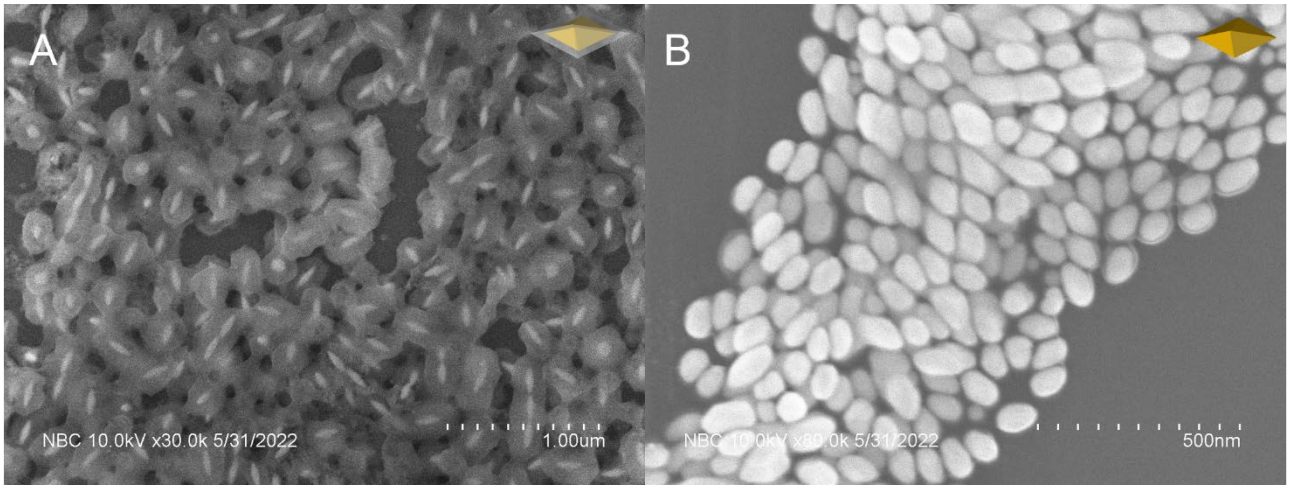

Figure 21. Reshaping phenomenon in (A) Au-NBPS@ZIF-8, (B) Au-NBPs.

2.3.3 Dynamic conditions

The VOC detection in dynamic conditions is more meaningful for our purposes with respect to the one carried out in saturation conditions, since it is closer to a real sensing circumstance. Therefore, it is worth to carry out experiments where the amount of analyte flowed through the chamber is controlled for different reasons. Firstly, in order to understand if the different samples are capable to detect the analyte even in unsaturated conditions. Secondly, to check the limit of detection of the different samples in terms of analyte concentration. Finally, these concepts can be pushed to the quantification of the amount of analyte in the atmosphere. Indeed, the amplitude of the reference Raman peak of the analyte could be associated to the ppm present in the analysed atmosphere. My samples, as shown in substrates preparation subsection, are quite homogeneous on the scale of the laser spot (~10μm), but based on my experience not totally reproducible. In order to take into account the possible inhomogeneities, the Raman spectra are acquired through a mapping tool, that allows the record of more Raman spectra in a designated zone, that are then averaged out. Concerning the first experiment, an atmosphere with 10% of toluene, corresponding to about 4000 ppm, is flowed through the chamber for a certain amount of time. After this, the presence of toluene is checked by

looking at its main peak at σ = 1004 cm^{-1} (Figure 22). It can be noticed that the presence of toluene is easy detectable with Au-NBPs and, albeit with more difficulties, also with Au-NBPs@ZIF-8. Instead, concerning Au-NBPs:ZIF-8, here the peak is practically not visible. This can be due to the fact that in this case the MOF traps the analyte far from the enhancement spots of the NPs, reasoning that can be particularly valid for the NBPs, indeed in this case the EM field is confined in the apices. Even in this case, as for the saturation condition measurements, it must be specified that the amplitude of the toluene main peak is meaningless since not properly re-normalized. Nevertheless, using the UV-VIS spectroscopy it would be possible to properly re-normalize the peak amplitude with respect to the absorbance (Appendix III. UV-Visible spectra of gold dispersions). In conclusion, we have demonstrated that is possible to detect toluene even in dynamic conditions with most of the substrates, paving the way for sensitivity measurements.

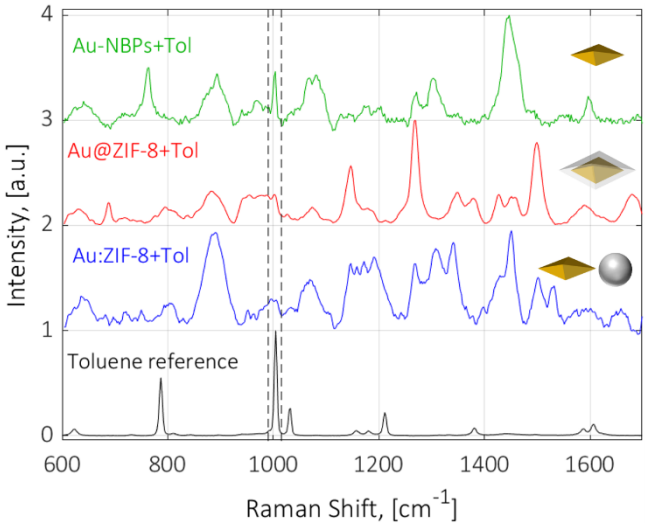

Figure 22. Raman spectra of different Au-NBPs & ZIF-8 substrates under a ~4000ppm toluene atmosphere.

3 Conclusion and perspectives

Finally, several conclusions can be drawn. First of all, we are capable to produce both UiO-66(NH_2), ZIF-8 and Au@ZIF-8 core-shells NPs. The MOFs of interest, namely ZIF-8 and UiO-66 (NH_2), turn out to have very good crystallinity, that is the most important feature to ensure the diffusion of the target analyte through the MOF pores. Au-NBPs@ZIF-8 turn out to be very well shaped, indeed the ZIF-8 covers completely and homogeneously the Au-NBPs. Secondly, we are able to prepare different substrates exploiting NPs with different morphologies and features. For Au-NPs, an aggregation in islands is observed but the islands are quite homogeneously dispersed. For both the MOFs we observed a uniform deposited layer, resulting in the best samples. Concerning Au@MOF core-shells, a good homogeneity can be noticed, despite the presence of some MOF particles alone due to homonucleation. Lastly, the Au:MOF composites turn out to slightly less homogeneous than other substrates. Nevertheless, a good dispersion of Au and MOF is obtained, and NPs aggregation is avoided. Lastly, the Raman sensing is still at the early stage, up to now we were able to check the detection of toluene with all the different samples in saturation conditions. Furthermore, the desorption of the analyte, as well as the stability of the sample during the desorption process itself, has been studied in order to ensure the reusability. Afterwards, the detection of toluene in dynamic conditions has been checked for different samples. Considering all the aforementioned achievements, this project has several perspectives. In particular, in the synthesis framework, the capability to produce core-shells using UiO-66(NH_2) as shell would pave the way for MOF performance comparison. Finally, concerning the Raman sensing, the major perspectives are represented by the estimation of sensitivity and selectivity of the different sensors made of the different substrates.

3.1 Sensitivity

The sensitivity of a sensor indicates how much its output changes when the input quantity it measures changes. Hence, the most performant sensor will be the one with higher sensitivity in the range of interest. It comes that it is of paramount importance to determine this quantity for two main reasons. Firstly, by determining the sensitivity of samples with different NPs and morphologies, one can have direct comparison of the sensor performances being able to determine the best one. Secondly, once the best sample would be determined, a calibration plot based in the linear range of sensing can be realized exploiting the sensitivity (the slope of this linear part, Figure 23B), leading to the possibility of analyte quantization for an unknown atmosphere under analysis.

To determine the sensitivity, the idea is to carry out experiments where atmospheres with different concentrations are flowed through the chamber and the amplitude of the analyte peak is monitored. In this way, for any concentration, an absorption curve can be retrieved (Figure 23A). For any concentration, the sample under study will start to adsorb/trap the analyte up to the establishment of a dynamic equilibrium that would stabilise the amplitude of the peak. This amplitude would be taken as “saturation” value for that concentration, and the sensitivity can be determined thanks to the measurement of this value for different concentrations.

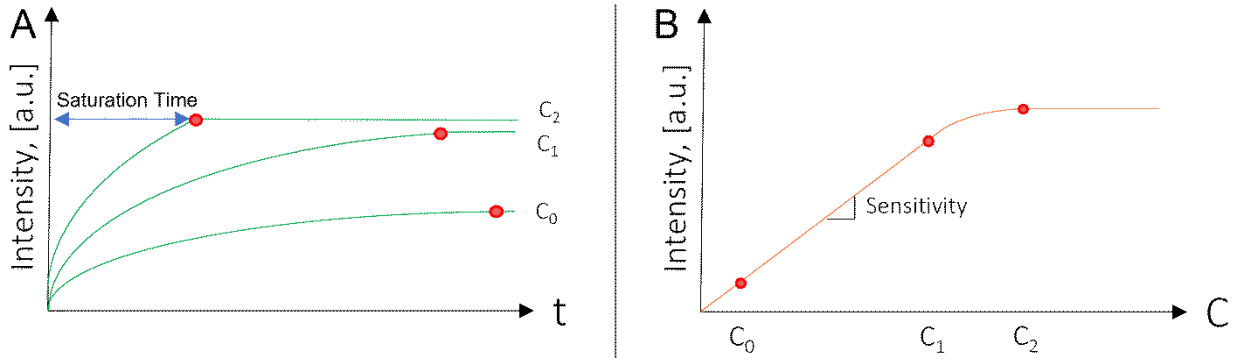

Figure 23. Schematic of: (A) Toluene absorption curves for different concentrations, (B) Toluene sensitivity curve.

3.2 Selectivity

The selectivity of this sensor is the ability to discriminate the target from other molecules present in the atmosphere and display a target-specific sensor response. The chemical versatility of the MOFs compounds and in particular the ZIF-8 hydrophobicity and the UiO-66(NH_2) hydrophilicity make them sensitive towards different molecules. We expect that a hydrophilic substance will be easily hosted by UiO-66(NH_2), whereas a hydrophobic one would chemically prefer to be hosted by ZIF-8. Therefore, if one is able to flow on a substrate an atmosphere containing both the types of analytes, it is expected to find a difference in the peak amplitude depending on the MOF we are flowing the atmosphere on (Figure 24).

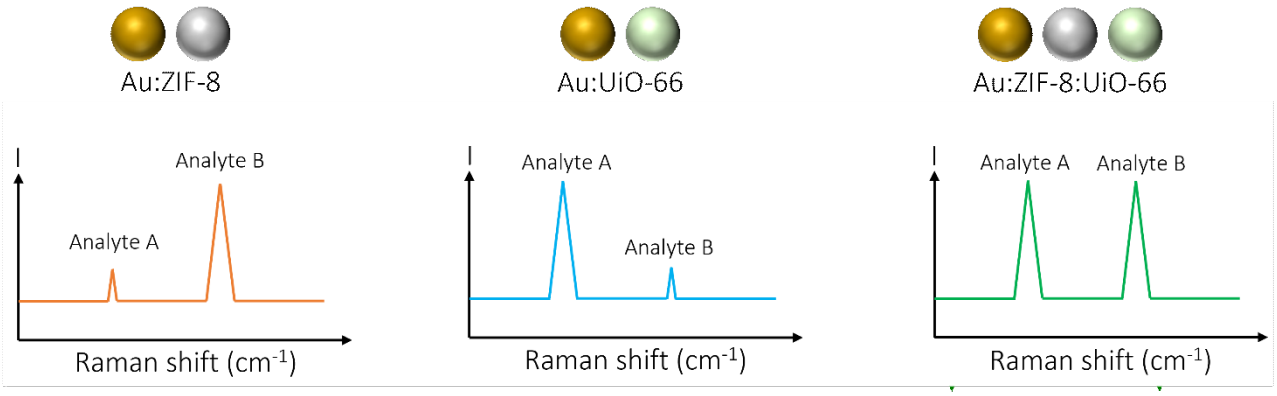

Figure 24. Schematic of expected Raman spectrum outcomes for substrates with different hydrophilicity.

Some preliminary investigations concerning the analytes have already been performed. Indeed, in order to detect an analyte, it must have at least one characteristic Raman peak that does not overlap with the ones of the MOFs one is going to use. Concerning the hydrophobic analyte, I already knew toluene was suitable for ZIF-8 so it is just checked the overlapping with UiO-66(NH_2) peaks. Instead, for the hydrophilic analyte the choice is little bit harder because it has to be miscible with toluene and non-toxic for human being to be compatible with our experimental setup. Among the non-toxic ones, isopropanol is well known to be absorbed in the UiO-66(NH_2) structure, but its main peak is overlapping the one of UiO-66(NH_2). Acetic acid could have been a VOC of interest, but it reacts with ZIF-8 producing zinc acetate. Therefore, the choice fell on ethanol which seems to have all the required features in terms of Raman spectrum and is miscible with toluene (required by the setup) (Figure 25).

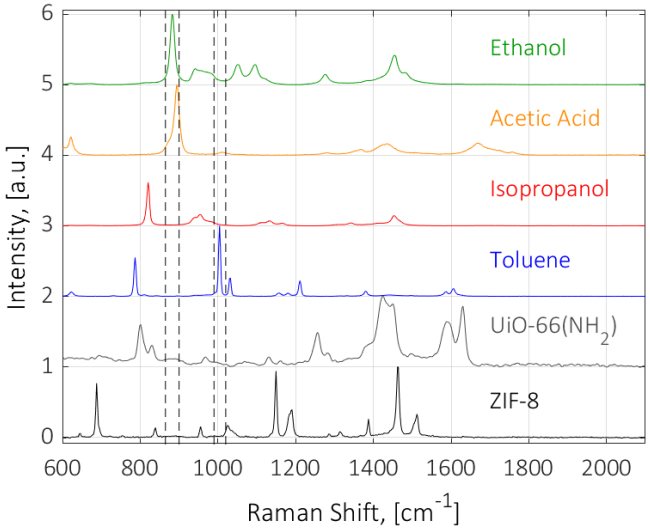

Figure 25. Raman spectra of different candidate analytes and both ZIF-8 and UiO-66(NH_2).

Appendices

I. Synthesis

I.A. ZIF-8

293 mg of $Zn(NO_3)_2$ are diluted in 120 mL of methanol. The same is dilution is performed for 649 mg of 2-methylimidazole. The two solutions are mixed together and stirred by means of magnetic stirrer for 1 hour at room temperature. After that, cleaning processes to remove the unreacted precursors are performed. Each cleaning process happens as follows. Firstly, the solution is centrifugated at $10x10^3$ rpm for 20 minutes to separate the composite from the solvent. Then the supernatant is withdrawn and the sticked preparate is dispersed in 40 mL of ethanol. Finally, the redispersion is performed thanks to 15 minutes sonication. After two cleaning processes the solution is again centrifugated with the same settings as in the cleaning processes and, once the supernatant is removed, the preparation is re-dispersed in 20 mL of ethanol. The re-dispersion is helped by 15 minutes sonication.

I.B. UiO-66(NH_2)

This synthesis is performed in two steps, in the first one $Zr_6O_4(OH)_4(CH_3CO_2)_{12}$ clusters are produced, in the second UiO-66 (NH_2) is obtained. The first step starts by diluting 1g of $ZrCl_4$ in 18 mL of isopropanol and 4 mL of acetic acid. The mixture is put in a round-bottom flask and brought to 90°C for two hours. The obtained product is redispersed in acetone and then centrifugated. Once the supernatant is removed, the remaining product is placed in a rotary evaporator from which the $Zr_6O_4(OH)_4(CH_3CO_2)_{12}$ clusters powder will be obtained. In this second step 300 mg of this powder are diluted in 2 mL of acetic acid and 5 mL of H_2O and the mixture is stirred up to transparency. Afterwards 20 mL of ethanol and 210 mg of 2-aminoterepthalic acid (BDC-NH_2) are added to the solution. The mixture is then stirred for two hours at room temperature and after is submitted to two cleaning processes as well as ZIF-8. In this case redispersing the solid part in a 35:5 mix of ethanol and water. After the last cleaning process, the mixture is centrifugated and redispersed in 30 mL of ethanol.

I.C. Au-NBPs@ZIF-8

542 mg of 2-methylimidazole (2-MeImdz) are diluted in 5 mL of H_2O and then stirred for 5 minutes at room temperature. The same stirring process is applied to 714 mg of $Zn(NO_3)_2$ diluted in 100 mL of H_2O. After that 36 μL of Cetyltrimethyl ammonium bromide (CTAB) water solution is mixed with 0,5 mL of 2-MeImdz solution, the mixture is then stirred for 5 minutes at room temperature. Afterwards, 0.5 mL of $Zn(NO_3)_2$ water solution are added and everything is stirred for 5 minutes at room temperature. 0.5 mL of Au-NBPs water dispersion are added and the solution is again stirred for 5 minutes at room temperature. The mixture is left to rest for 1 hour and then 3 cleaning processes as well as for ZIF-8 are performed using 5 ml of ethanol for each redispersion. Finally the solution is centrifugated at $10x10^3$ one last time and the solid part is redispersed in 3.5 mL of ethanol.

II Characterization

II.A. XRD

X-Ray Diffraction is an analysis technique based on the diffraction of X-rays by matter. This technique is used on crystalline samples and makes it possible to obtain information on the dimensions of the crystal lattice, the space group as well as the position of the atoms in the lattice. X-rays are created in an X-ray tube by bombarding a target material with very high energy electrons, photons or protons. These X-rays will then be directed towards the sample where elastic scattering will take place. The ray will then be collected by a sensor and then analysed. The directions and intensities of the diffracted rays directly depend on the nature of the position of the atoms in the crystal under analysis. This technique can be used to build the structure of any crystalline compound from the angles of deflection of the rays. During this internship, I used XRD to know the structure of the different synthesized compounds: ZIF-8, UiO-66 (NH2) and Au-NBPs@ZIF-8. Powder X-ray diffraction (XRD) measurements were performed on a Bruker D8 Advance diffractometer at Cu Kα radiation (λ = 1.5409 Å) with a LynxEye XE-T detector.

II.B. TEM

Transmission Electron Microscopy is an analytical technique to image very thin specimen at the nanoscale. The light sources are electrons produced by a heated tungsten filament, they are then accelerated and focused on the sample thanks to electromagnetic lenses. A very strong vacuum in the column generates a very low pressure to avoid the electrons to collide with gas molecules which could make them deviate from the trajectory. The electrons created from the filament will cross the specimen and be collected on a screen which will become fluorescent following the bombardment of the electrons. The operator will be able to access the image formed on this screen. During this internship, transmission electron microscopy was used to characterize the size and morphology of the products of our different syntheses, such as ZIF-8, UiO-66 (NH2) and Au-NBPs@ZIF-8. High-resolution transmission electron microscopy (HR-TEM) was performed on an FEI Titan Themis microscope operating at 300 kV with a Falcon3 EC 4k/4k Direct Detection Electron (DDE) camera.

II.C. SEM

Scanning Electron Microscopy is an analytical technique used to image surfaces at the nanoscale. The light sources are electrons produced by a heated tungsten filament or by a field emission gun tip, then they are accelerated and focused on the sample by means of electromagnetic lenses. A very strong vacuum in the column generates a very low pressure to avoid the electrons to collide with gas molecules which could make them deviate from the trajectory. The electrons will interact with the atoms at the sample surface producing various signals that contain information about the surface topography and the chemical composition of the sample. These signals are collected by different detectors and then are software-elaborated. During this internship, scanning electron microscopy was used to characterize the surface topography of all the solutions that have been deposited, namely Au-NPs, MOFs, Au@MOF, Au:MOF. Scanning electron microscopy (SEM) images were obtained on a HitachiS4800 microscope with a field emission electron gun at 5 kV.

II.D. Raman Spectroscopy

Raman Spectroscopy is a non-destructive chemical analysis technique which provides detailed information about chemical structure, phase and polymorphy, crystallinity and molecular interactions. It is based upon the interaction of light with the chemical bonds within a material. Raman is a light scattering technique, whereby a molecule scatters incident light from a high intensity laser light source. Most of the scattered light is at the same wavelength as the laser source and does not provide useful information. However a small amount of light is scattered at different wavelengths, which depend on the chemical structure of the analyte. A Raman spectrum features a number of peaks, showing the intensity and wavelength position of the Raman scattered light. Each peak corresponds to a specific molecular bond vibration, polymer chain vibrations, lattice modes, etc. Therefore, typically a Raman spectrum is a distinct chemical fingerprint for a particular molecule or material, and can be used to very quickly identify the material, or distinguish it from others. During the internship, I have used this spectroscopy technique to

verify the chemical composition of synthetised MOFs, and mostly to detect and identify VOCs. Raman spectroscopy was performed on a Horiba LabRam HR evolution spectrometer.

III. UV-Visible spectra of gold dispersions

The quantitative comparison about the capability of different substrates of detecting analytes is a desirable goal to evaluate which way to combine Au-NPs and MOF is the most performant and efficient one. In order to do that, we want to be able to compare the amplitudes of the main peak of a certain analyte (under the same exposition condition to the analyte itself) detected by two different samples. Now, assuming that we use the same Raman acquisition parameters, the same size and shape of the Au-NPs and a good deposition homogeneity, the only difference between the substrates will be the local concentration of Au-NPs. If one would be able to know the concentration of the starting solution, the local concentration could be retrieved and the amplitudes of the Raman peak under the aforementioned conditions could be renormalized with respect to the concentration. Unfortunately, we are not able to determine the concentration of Au neither in Au-NPs alone solutions nor in Au@MOF core shell solution. Nevertheless, for diluted solutions, the absorbance is proportional to the concentration of NPs through the molar extinction coefficient and the crossed thickness of solution. Therefore, by performing the UV-VIS spectroscopy for both the Au-NPs alone and the Au-NPs@MOF solutions (using as precursor for the core-shell the same Au-NPs to keep constant the molar extinction coefficient!) it is possible to re-normalize the amplitude of the peaks with respect to the absorbance. Since for the composites the concentration will be the one of Au-NPs alone, this reasoning holds also them. This re-normalization allows the comparison between the performances of Au-NPs, Au-NPs@MOF and Au-NPs:MOF substrates, enabling the possibility to understand if the use of MOFs provide advantages and, if yes, in which configuration of mixing with Au-NPs it provides the more. Up to now we only have the UV-VIS spectra of Au-NBPs (Figure III.1), in the next month the ones of core-shells will be acquired allowing us to perform this kind of analysis.

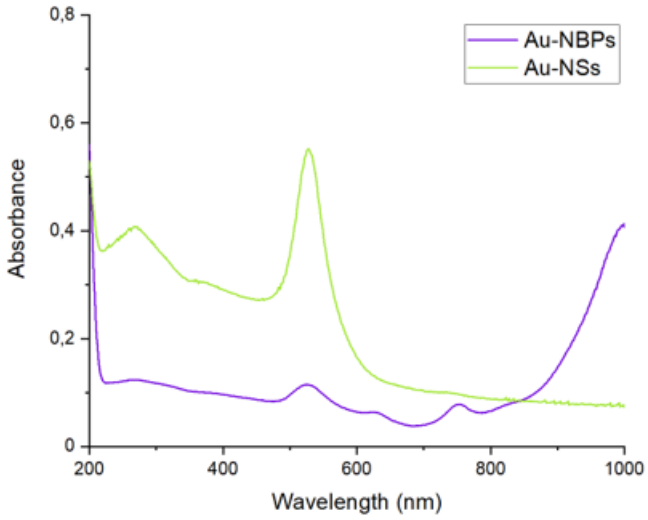

Figure III.126. Absorbance spectra of Au-NSs and Au-NBPs.

References

1. Langer, J. *et al.* Present and future of surface-enhanced Raman scattering. *ACS Nano* **14**, 28–117 (2020).

2. Sánchez-iglesias, A., Winckelmans, N., Bals, S., Grzelczak, M. & Liz-marzán, L. M. High Yield Seeded Growth of Monodisperse Pentatwinned Gold Nanoparticles Through Thermally-Induced Seed Twinning. *J. Am. Chem. Soc.* **139**, 107–110 (2017).

3. Sánchez-Iglesias, A. *et al.* Synthesis and optical properties of gold nanodecahedra with size control. *Adv. Mater.* **18**, 2529–2534 (2006).

4. Dai, S., Nouar, F., Zhang, S., Tissot, A. & Serre, C. One-step versatile room temperature synthesis of metal(IV) carboxylate MOFs. *Angew. Chemie Int. Ed.* (2020) doi:10.1002/anie.202014184.

5. Dai, S., Nouar, F., Zhang, S., Tissot, A. & Serre, C. One-Step Room-Temperature Synthesis of Metal(IV) Carboxylate Metal—Organic Frameworks. *Angew. Chemie - Int. Ed.* **60**, 4282–4288 (2021).

6. Lafuente, M. *et al.* Plasmonic MOF Thin Films with Raman Internal Standard for Fast and Ultrasensitive SERS Detection of Chemical Warfare Agents in Ambient Air. *ACS Sensors* (2021).

7. Yang, X. *et al.* Site-Selective Deposition of Metal-Organic Frameworks on Gold Nanobipyramids for Surface-Enhanced Raman Scattering. *Nano Lett.* **21**, 8205–8212 (2021).

8. Chen, Q. Q. *et al.* Au@ZIF-8 Core-Shell Nanoparticles as a SERS Substrate for Volatile Organic Compound Gas Detection. *Anal. Chem.* **93**, 7188–7195 (2021).

9. Liu, Y. *et al.* Core-shell noble-metal@metal-organic-framework nanoparticles with highly selective sensing property. *Angew. Chemie - Int. Ed.* **52**, 3741–3745 (2013).

10. Koh, C. S. L., Lee, H. K., Han, X., Sim, H. Y. F. & Ling, X. Y. Plasmonic nose: Integrating the MOF-enabled molecular preconcentration effect with a plasmonic array for recognition of molecular-level volatile organic compounds. *Chem. Commun.* **54**, 2546–2549 (2018).

11. Phan-Quang, G. C. *et al.* Tracking airborne molecules from afar: Three-dimensional metal-organic framework-surface-enhanced raman scattering platform for stand-off and real-time atmospheric monitoring. *ACS Nano* **13**, 12090–12099 (2019).

12. Dedecker, K. Multifunctional hybrid materials for the capture and detection of VOCs_Application to the preservation of cultural heritage objects.pdf. (2019).

13. Cavka, J. H. *et al.* A new zirconium inorganic building brick forming metal organic frameworks with exceptional stability. *J. Am. Chem. Soc.* **130**, 13850–13851 (2008).

14. Guillerm, V. *et al.* A zirconium methacrylate oxocluster as precursor for the low-temperature synthesis of porous zirconium(iv) dicarboxylates. *Chem. Commun.* **46**, 767–769 (2010).

15. Schaate, A. *et al.* Modulated synthesis of Zr-based Metal-Organic Frameworks: From nano to single crystals. *Chem. Eur. J.* **17**, 6643–6651 (2011).